Source Reconstruction Method based on Machine Learning Algorithms

He Ming Yao, Lijun Jiang
Department of Electrical and Electronic Engineering
The University of Hong Kong, Hong Kong, China
yaohmhk@hku.hk, jianglj@hku.hk

Wei E.I. Sha
College of Information Science & Electronic Engineering
Zhejiang University, Hangzhou, China
weisha@zju.edu.cn

***Abstract*—This paper proposes a new source reconstruction method (SRM) based on deep learning. The conventional SRM usually requires oversampled measurements data to ensure higher accuracy. Thus, conventional SRM numerical system is usually highly singular. A deep convolutional neural network (ConvNet) is proposed to reconstruct the equivalent sources of the target to overcome difficulty. The deep ConvNet allows us to employ less data samples. Besides, the ill-conditioned numerical system can be effectively avoided. Numerical examples are presented to demonstrate the feasibility and accuracy of the proposed method. Its performance is also compared with the traditional neural network and interpolation method. Moreover, we further expand the proposed method to measure the permittivity of dielectric scatterers.**

Keywords—source reconstruction method, convolutional neural network, machine learning

I. INTRODUCTION

The source reconstruction method (SRM) can employ integral equations to construct equivalent source distributions of target objects from the near field (NF) or far field (FF) measurements [1]. By using the scattered field in the observation domain, the distribution of sources on an object can be approximated. The reconstructed sources can be utilized for source error test, hot-spot identification, NF to FF transformations [1-2], etc. In the past few decades, reconstruction algorithms have been proposed, such as Born approximation method [3], Bayesian probability method [4], compressive sensing [5], and other deterministic algorithms [6]. However, all these conventional approaches encounter solving singular numerical systems, which makes SRM a complicated computational challenge [1-2].

Employing machine learning (ML) in advanced computational electromagnetics and relevant applications have been initiated long time ago [7-8]. Due to recent blooming learning technologies, the convolutional neural network (ConvNet) [9] has become one of the most important new methods in deep learning applications. For example, ConvNet has been widely used in imaging processes [9].

In this paper, we propose to employ a deep ConvNet for the source reconstruction process. The advantages of the proposed method are: (1) the proposed deep ConvNet model allows calculation using much less field samples than the conventional SRM; (2) the proposed method avoids handling a singular numerical system because the inverse solving process of conventional SRM is avoided; (3) the proposed deep ConvNet approach can make far field information to do reconstruction; (4) the proposed method has satisfactory accuracy and superior performance over traditional neural networks and interpolation methods [10-11].

Compared to the traditional neural networks (NNs) and interpolation method [10-11], ConvNet can more efficiently map the relations between inputs and outputs mainly by convolutional layer and activation layer [12]. Thus, unlike traditional NNs, ConvNet does not need very large number of neural units to handle problems [12]. The specific comparison between different methods is provided in Section III.

The paper is organized as follows: In Section II, the source reconstruction formulation is briefly reviewed, followed by a description of the proposed ConvNet structure. Then, the proposed ConvNet method for solving source reconstruction problems is proposed. In Section III, numerical examples are provided to present the validity and precision of the proposed method, which are also compared with the results obtained by interpolation method and backpropagation neural network. Finally, the conclusion is shown in Section IV.

II. FORMULATON AND THEORY

A. Problem Formulation

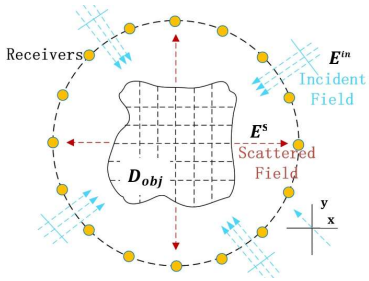

Fig. 1. Schematic of Scattering Scenario

The representative 2D equivalent current density reconstruction, as shown in Fig. 1, is used to demonstrate the procedures of our methodology. In Fig. 1, D_{obj} is a dielectric area, denoting the domain of interest. It is divided into n=1,2,…N patches. The transverse magnetic (TM) incidence plane wave is denoted as $\boldsymbol{E}^{in}$. The scattered field $\boldsymbol{E}^{s}$ in z direction can be represented by z direction current density as:

$$E^s(\boldsymbol{r}) = -j\omega\mu_0 \int g(\boldsymbol{r},\boldsymbol{r}')J_s(\boldsymbol{r}')d\boldsymbol{r}' \qquad (1)$$

where $g(\boldsymbol{r},\boldsymbol{r}')$ is the scalar Green's function. For TM wave, it can be defined as $g(\boldsymbol{r},\boldsymbol{r}') = -\frac{j}{4}H_0^{(2)}(k_0|\boldsymbol{r}-\boldsymbol{r}'|)$. $H_0^{(2)}$ stands for the second-kind Hankel function of zero$^{\text{th}}$ order. $\boldsymbol{r} = (x,y)$ and $\boldsymbol{r}' = (x',y')$ are the field and source points,

respectively. $\boldsymbol{J}_s$ is the equivalent current density on the target object D_{obj}.

According to the Lippmann–Schwinger equation [13], the relationship between the incident electrical field $\boldsymbol{E}^{in}$ and equivalent current density distribution $\boldsymbol{J}_s$ on D_{obj} is presented as:

$$E^{in}(\boldsymbol{r}) - j\omega\mu_0 \int g(\boldsymbol{r},\boldsymbol{r}')J_s(\boldsymbol{r}')d\boldsymbol{r}' = \frac{J_s(\boldsymbol{r})}{j\omega\ {}_0(\varepsilon_r - 1)} \qquad (2)$$

where ε_0 and μ_0 are the vacuum permittivity and permeability, and ε_r is the relative permittivity of D_{obj}.

It has been widely acknowledged that the property of object can be characterized by its equivalent current density distribution $\boldsymbol{J}_s$. For different incident angles β_l of $\boldsymbol{E}^{in}$ (l=1….L) and different receivers in the far field at measurement angles φ_m (m=1…M), the relationship between the scattered field $\boldsymbol{E}^s$ and equivalent current density $\boldsymbol{J}_s$ is:

$$E^s(\varphi_m,\beta_l) = -j\omega\mu_0 \sum_{n=1}^{N} g(\varphi_m,\boldsymbol{r}'_n)J_{s,n}^{\beta_l} A_n \qquad (3)$$

where A_n is the equivalent area of n$^{\text{th}}$ divided D_{obj} fragment and $J_{s,n}^{\beta_l}$ is the equivalent current density on the n^{th} piece with the incident field angle β_l.

The aim of conventional reconstruction methods is utilizing $E^s(\varphi_m,\beta_l)$ to obtain $J_{s,n}^{\beta_l}$. However, in the conventional process, numerous φ_m has to be used to retrieve $J_{s,n}^{\beta_l}$, which could be ill-conditioned [1-2]. Hence, Conventional SRM suffer from the expensive calculation cost and relatively low accuracy.

B. Integration of ConvNet to Source Reconstruction

A deep ConvNet is proposed to replace the conventional SRM. The architecture of the proposed ConvNet is shown in Fig. 2. Thus, we can rewrite the source reconstruction process in a simplified form as (4):

$$\begin{cases} \mathbf{Y} = F(\mathbf{X};\boldsymbol{\Theta}) \\ \mathbf{X} = \mathbf{E}^s \\ \mathbf{Y} = \mathbf{J}_s \end{cases} \qquad (4)$$

where for each β_l, $\mathbf{E^s} = [E^s(\varphi_1,\beta_l),\dots,E^s(\varphi_M,\beta_l)]$ and $\mathbf{J_s} = \left[J_{s1}^{\beta_l},\dots J_{s,n}^{\beta_l},\dots J_{sN}^{\beta_l}\right]$. The mapping F represents the equivalent source reconstruction process based on the ConvNet. $\boldsymbol{\Theta}$ is the parameters of the ConvNet (weights and biases).

The modeling procedure by using our deep ConvNet is as follows: (1) Training data collection: the known $\mathbf{J}_s$ under different incident waves and its resultant $\mathbf{E}^s$ are collected through direct forward computations to form training data set. (2) Training ConvNet: we use $\mathbf{E}^s$ as the input of proposed ConvNet (real and imaginary part) while $\mathbf{J}_s$ (real and imaginary part) act as the output. we have L groups of input and output of proposed ConvNet. Based on these data, we start to train ConvNet F; (3) Reconstructing source: based on the resultant ConvNet, we can then reconstruct $\mathbf{J}_s$ illuminated by new incident waves. Because of the advantages of ConvNet, the proposed method can reconstruct equivalent current even with less complexity (smaller M) and good accuracy. The regularization technique is adopted to reduce overfitting and decrease the complex of model. Then, our trained deep ConvNet model can be used to realize source reconstruction for unknown situation. The performance of the ConvNet is discussed in the following Sections.

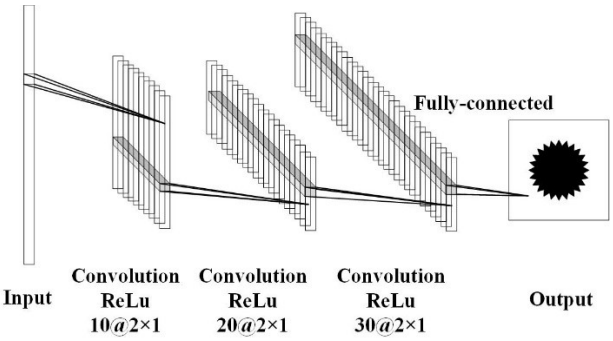

Fig. 2. ConvNet architecture for the source reconstruction

In the internal architecture of proposed ConvNet, the convolutional layer and activation layer unit operates to capture features of input. Convolutional layer number, kernel number f, its size K, and the stride for kernel are shown in Table I. Then, this convolutional layer and activation layer unit feed into a final fully-connected layer, which is the prediction of the reconstructed source. This final output is also used to compute the mean-squared error between the true label and the predicted label, referred to as the loss.

The proposed method is benchmarked in Matlab 2018b with Deep Learning Toolbox [14]. The mean-squared error loss function is optimized by the stochastic gradient descent. The learning rate, chosen as 0.01, is the hyper-parameter in our model. We can control training error by declining the learning rate. The training is done by full batch. L2 regularization is applied to prevent over-fitting and improve prediction accuracy [15].

TABLE I
CONVNET ARCHITECTURE

Type	Filter Number	Filter Size	Stride	Input Size	Output Size
Convolution	10	2×2	2	M×2×1	(M/2)×1×10
ReLu				(M/2)×1×10	(M/2)×1×10
Convolution	20	2×1	1	(M/2)×1×10	(M/2)×1×20
ReLu				(M/2)×1×20	(M/2)×1×20
Convolution	30	2×1	1	(M/2)×1×20	(M/2)×1×30
ReLu				(M/2)×1×30	(M/2)×1×30
Fully-connected Regression				(M/2)×1×30	N×2

III. NUMERICAL RESULTS

Several numerical examples and application scenarios are used to demonstrate the proposed source reconstruction method.

A. Reconstruction for an Arbitrary Single Object

A 2D Z-shaped dielectric object is firstly used to demonstrate the performance of the proposed ConvNet method, as shown in Fig. 3.

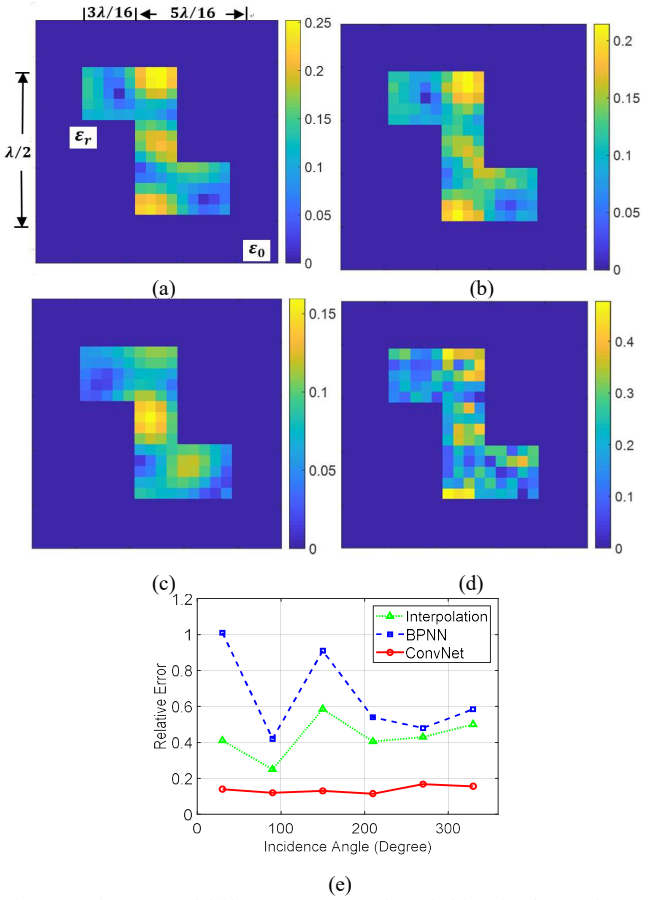

Fig. 3. Performance of different SRM on Z-shaped object for β=270 degree. (a) Known accurate numerical current distribution. (b) Current distribution calculated from the ConvNet prediction. (c) Current distribution calculated from the nearest interpolation method. (d) Current distribution calculated from conventional BPNN. (e) Relative error Comparison between ConvNet, BPNN, the interpolation on different incident angles.

In Fig. 3(a-d), the wavelength λ of incident TM_z wave is 1 meter, the dielectric permittivity of object ε_r is 8, and its geometric parameters are shown in Fig. 3(a). The source current density $\mathbf{J}_s$ is assumed to be distributed on an artificial grid 24×24, (N=576). The $\mathbf{E}^s$ are collected along 10 equally spaced directions (M=10) as the input of the training data. Only 6 equally spaced incident directions (β = 0°, 60°, …., 300°) for $\boldsymbol{E}^{in}$ are used to stimulate the object to get the training data. The nearest interpolation method is used for the comparison. We also use a traditional Back Propagation Neural Network (BPNN) to reconstruct the source [10], of which the training data are also $\mathbf{E}^s$ as input and $\mathbf{J}_s$ as output. The structure of BPNN has three layers: input, hidden-layer and output layer. There are 20 hidden-layer units of hyperbolic tangent basis function.

Then, six new incident angles (β =30°, 90°…330°) are utilized to obtain new induced current and scattered field $\mathbf{J}_s$ and $\mathbf{E}^s$ from the Z-shaped object. $\mathbf{E}^s$ is used as the input of the trained ConvNet to reconstruct the equivalent source. The resultant source is further compared with $\mathbf{J}_s$ to verify its accuracy. Fig. 3 (b-d) present the reconstructed source for the incident angle β = 270° case only. It is evident that the ConvNet has the highest precision while the traditional BPNN provides the worst result.

The performance of all six new incident cases are given in Fig. 3(e). The accuracy relative to the original $\mathbf{J}_s$ is computed by the relative error in equation (5):

$$e = \frac{\| |\mathbf{J}_{S,SRM}| - |\mathbf{J}_{S,acc}| \|}{\|\mathbf{J}_{S,acc}\|} \quad (5)$$

where $\mathbf{J}_{S,SRM}$ is the current density computed from source reconstruction processes and $\mathbf{J}_{S,acc}$ is the original current density distribution computed directly from the incident wave.

We can see that the propose ConvNet always has the smaller error (below 0.2) than that of interpolation method (about 0.4), while BPNN has the worst performance for all testing situations.

B. Reconstruction for Multi-Objects

The performance of the proposed ConvNet for multi-objects in D_{obj} is presented in this section. With all similar setups including those for comparisons, only the Z-shaped object is replaced by two different squares.

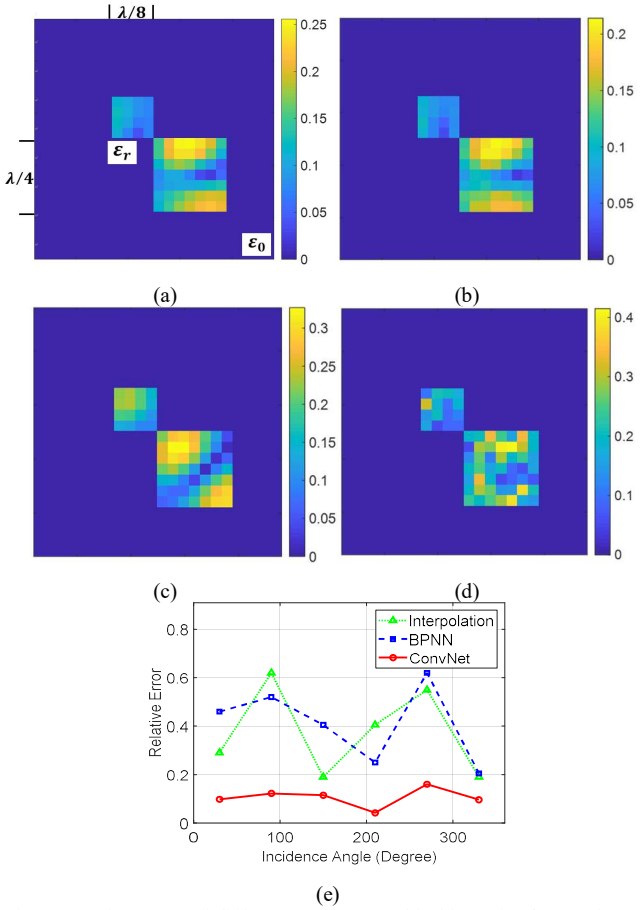

Fig. 4. Performance of different SRM on multi-objects for β=270 degree. (a) Known accurate numerical current distribution. (b) Current distribution calculated from the ConvNet prediction. (c) Current distribution calculated from the nearest interpolation method. (d) Current distribution calculated from conventional BPNN. (e) Relative error Comparison between ConvNet, BPNN, the interpolation on different incident angles.

The results are the same as that in Section III A. Fig.4(b-d) shows the predicted result from different methods. It is evident that the ConvNet has the highest accuracy while the traditional BPNN nearly fails in reconstructing the equivalent

source or providing meaningful information. From Fig.4(e), we can also see that the proposed ConvNet always has the smaller error (below 0.2) than other two methods.

C. New Permittivity Measurement Approach

The proposed method can be a new methodology for the permittivity measurement. Conventional method requires specific reflection or transmission measurements based on special test fixtures and equipments [16]. By using our proposed deep ConvNet model, the permittivity measurement can become a much flexible scattered field data acquisition process. The proposed new process is as follows: (1) Collecting measurement model training data: we use TM_z incident wave in a certain direction to illuminate the homogeneous dielectric object with a certain shape. The scattered field $\mathbf{E}^s$ are collected at a fixed range and several angles. $\mathbf{E}^s$ will be used as the training input and the object's permittivity ε_r will be used as the training output. We then change ε_r but keep the same incident field to get another group $\{\mathbf{E}^s, \varepsilon_r\}$ as another set of training data. (2) Train the ConvNet model for the permittivity measurement: by using the training data collected in step one, a new ConvNet is trained to predict the permittivity based on the scattered field $\mathbf{E}^s$; (3) Permittivity measurement: when an unknown dielectric is under test, it will be made into the same shape used for training objects first. Then it is illuminated by the incident wave same to that for the training in Step 1. Then the scattered field $\mathbf{E}^s$ is measured at the mentioned fixed range and given angles in Step 1. By inputting the measured $\mathbf{E}^s$ to the trained ConvNet, the unknown permittivity ε_r can be predicted by the model. the newly proposed approach is shown in Fig. 5. We here use the Z-shaped in Section III A as target object D_{obj}. The dielectrics with the permittivity (1.5, 2, 2.5, …, 6.5) are used to obtain the training data.

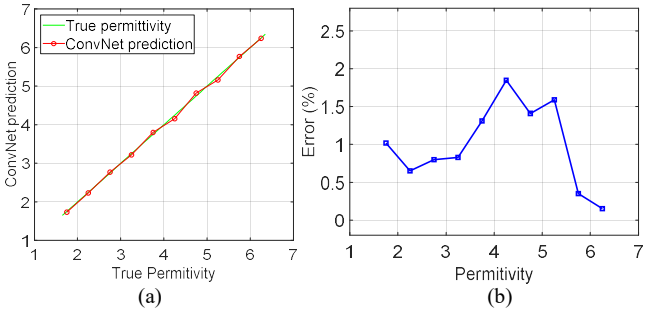

Fig. 5. Permittivity measurement results from ConvNet. Circles and squires are for the testing cases that have the permittivities different from the training cases. (a) Comparison between real permittivity and ConvNet prediction results. (b) Error of ConvNet prediction results

From Fig 5, we can see that the ConvNet can very accurately predict the permittivity, and the error of the studied results can be controlled below 2%.

IV. Conclusion

In this paper, we propose a new source reconstruction method using the deep ConvNet. The scattered fields resulting from incident waves of different incident angles are used as the input training data to the ConvNet while the induced current distributions are used as the output data. After the training, proposed ConvNet serves as the SRM engine to reconstruct the equivalent sources efficiently. Because of the merit of ConvNet, the newly proposed approach achieves better performance on the source reconstruction problem. The ConvNet model is further extended to propose a new permittivity measurement method. Several numerical examples are used to demonstrate the feasibility and accuracy of proposed ConvNet. We also compare the proposed ConvNet model with traditional neural networks and interpolation method to show the validity and advantages of our model. Our work offers a new way to leverage machine learning approaches for source reconstruction applications.

Acknowledgment

This work was supported in part by the Research Grants Council of Hong Kong GRF 17209918, AOARD FA2386-17-1-0010, NSFC 61271158, and HKU Seed Fund 201711159228.

References

[1] Y. Alvarez, F. Las-Heras and M. R. Pi no, "Reconstruction of Equivalent Currents Distribution Over Arbitrary Three-Dimensional Surfaces Based on Integral Equation Algorithms," *IEEE Trans. Antennas Propag.*, vol. 55, no. 12, pp. 3460-3468, Dec. 2007.

[2] Y. Alvarez, F. Las-Heras and M. R. Pino, "On the Comparison Between the Spherical Wave Expansion and the Sources Reconstruction Method," *IEEE Trans. Antennas Propag.*, vol. 56, no. 10, pp. 3337-3341, Oct. 2008.

[3] W. C. Chew, Y. M. Wang, G. Otto, D. Lesselier, J. C. Bolomey, "On the inverse source method of solving inverse scattering problems", *Inverse Problems*, vol. 10, pp. 547-552, 1994.

[4] Y. Yu, L. Carin, "Three-dimensional Bayesian inversion with application to subsurface sensing", *IEEE Trans. Geosci. Remote Sens.*, vol. 45, no. 5, pp. 1258-1270, May 2007.

[5] M. S. Chen, F. L. Liu, H. M. Du, X. L. Wu, "Compressive sensing for fast analysis of wide-angle monostatic scattering problems", *IEEE Antennas Wireless Propag. Lett.*, vol. 10, pp. 1243-1246, 2011.

[6] R. E. Kleinman, P. M. van den Berg, "Two-dimensional location and shape reconstruction", *Radio Sci.*, vol. 29, pp. 1157-1169, July-Aug. 1994.

[7] H. H. Zhang, H. M. Yao, and L. J. Jiang, "Embedding the behavior macromodel into TDIE for transient field-circuit simulations," *IEEE Trans. Antennas Propag.*, vol. 64, no. 7, pp. 3233–3238, Jul. 2016.

[8] H. Yao, L. Jiang and Y. Qin, "Machine learning based method of moments (ML-MoM)", *2017 IEEE International Symposium on Antennas and Propagation & USNC/URSI National Radio Science Meeting*, Jul. 2017.

[9] A. Krizhevsky, I. Sutskever and G. Hinton, "ImageNet classification with deep convolutional neural networks", *Communications of the ACM*, vol. 60, no. 6, pp. 84-90, 2017.

[10] R. G. Ayestarn and F. L. Heras, "Neural networks and equivalent source reconstruction for real antenna array synthesis, " *Electron. Lett.* vol. 39, no. 13, pp. 956-958, 2003.

[11] N. Hoang, "On node distributions for interpolation and spectral methods", *Mathematics of Computation*, vol. 85, no. 298, pp. 667-692, 2015.

[12] C. Dong, C. Loy, K. He and X. Tang, "Image Super-Resolution Using Deep Convolutional Networks", *IEEE Transactions on Pattern Analysis and Machine Intelligence*, vol. 38, no. 2, pp. 295-307, 2016.

[13] M. A. Fiddy and R. S. Ritter, *Introduction to Imaging from Scattered Fields*, CRC Press, 2014.

[14] P. Kim, *MATLAB deep learning*, Apress, 2017.

[15] A.Y. Ng, "Feature Selection L1 vs. L2 Regularization and Rotational Invariance", *Proc. 21st Int'l Conf. Machine Learning*, pp. 78-86, 2004.

[16] W. B. Weir, "Automatic measurement of complex dielectric constant and permeability at microwave frequencies", *Proceedings of the IEEE*, pp. 33-36, 1974.